Molecular-dynamics study on characteristics of energy and tangential momentum accommodation coefficients

Hiroki Yamaguchi,[1,*] Yu Matsuda,[2] and Tomohide Niimi[1]

[1]*Department of Micro-Nano Mechanical Science and Engineering, Nagoya University, Furo-cho, Chikusa, Nagoya, Aichi, 464-8603, Japan*

[2]*Institute of Materials and Systems for Sustainability, Nagoya University, Furo-cho, Chikusa, Nagoya, Aichi, 464-8603, Japan*

(Received 11 April 2017; revised manuscript received 15 June 2017; published 25 July 2017)

Gas-surface interaction is studied by the molecular dynamics method to investigate qualitatively characteristics of accommodation coefficients. A large number of trajectories of gas molecules colliding to and scattering from a surface are statistically analyzed to calculate the energy (thermal) accommodation coefficient (EAC) and the tangential momentum accommodation coefficient (TMAC). Considering experimental measurements of the accommodation coefficients, the incident velocities are stochastically sampled to represent a bulk condition. The accommodation coefficients for noble gases show qualitative coincidence with experimental values. To investigate characteristics of these accommodation coefficients in detail, the gas-surface interaction is parametrically studied by varying the molecular mass of gas, the gas-surface interaction strength, and the molecular size of gas, one by one. EAC increases with increasing every parameter, while TMAC increases with increasing the interaction strength, but decreases with increasing the molecular mass and the molecular size. Thus, contradictory results in experimentally measured TMAC for noble gases could result from the difference between the surface conditions employed in the measurements in the balance among the effective parameters of molecular mass, interaction strength, and molecular size, due to surface roughness and/or adsorbed molecules. The accommodation coefficients for a thermo-fluid dynamics field with a temperature difference between gas and surface and a bulk flow at the same time are also investigated.

DOI: 10.1103/PhysRevE.96.013116

I. INTRODUCTION

Along with the recent development of microscale and nanoscale technologies, microscale flows are gaining significance. In such microscale flows, especially in gaseous flows, the Knudsen number, defined by the ratio of the molecular mean free path to the characteristic length of a system, is an important parameter. Because of the size of the flow field, the Knudsen number becomes large; the flow is called a high Knudsen number flow. In high Knudsen number flows, the collision number of molecules to wall surfaces cannot be neglected compared to that between molecules in the fluid. In addition, the surface-to-volume ratio of the fluid is large due to the small size. Therefore, the gas-surface interaction plays an important role in microscale gaseous flows. The amounts of the velocity slip and temperature jump phenomena in the slip flow regime are determined by the gas-surface interaction [1].

To represent the gas-surface interaction, the accommodation coefficient is often employed. The accommodation coefficient is defined as

$$\alpha = \frac{\overline{\zeta_i} - \overline{\zeta_r}}{\overline{\zeta_i} - \overline{\zeta_s}}, \tag{1}$$

where ζ is a physical property of molecules and the overline represents the averaging over all concerned molecules. The subscripts i, r, and s denote the incident condition, the reflected condition, and the condition fully accommodated to a surface. This coefficient represents the mean degree of accommodation of each physical property of molecules to a surface. The size of the accommodation coefficient is known to differ by physical properties of molecules, like energy and momentums.

The accommodation coefficient on the energy is called the energy accommodation coefficient (EAC) [2,3], and it is defined as

$$\alpha_E = \frac{\overline{E_i} - \overline{E_r}}{\overline{E_i} - \overline{E_s}}, \tag{2}$$

where E denotes the energy of molecules. This coefficient is related to heat transfer between gas and surface. If there is no flow, namely the static condition, the energy of the molecules can be expressed by using temperature T as $\overline{E} = 2kT$, where k is the Boltzmann constant, and this coefficient can be expressed by T instead of E, which is called the thermal accommodation coefficient. EAC has been experimentally measured from the heat transfer through gas confined between two surfaces with different temperatures [2–7]. A typical measurement technique is the low-pressure method: The accommodation coefficient is deduced from the measurement of the heat flux through gas in the free-molecular flow regime as a function of pressure, because the heat flux is proportional to the number density of molecules, namely pressure, and the accommodation coefficients. It is important to note that the heat flux is measured without flow in the measurement system.

The tangential momentum accommodation coefficient (TMAC) [8,9] is also often employed to understand resistance to flow by surfaces. Since the condition fully accommodated to a surface $\overline{p_{t,s}} = 0$, it is defined as

$$\alpha_t = \frac{\overline{p_{t,i}} - \overline{p_{t,r}}}{\overline{p_{t,i}}}, \tag{3}$$

where p_t denotes the tangential momentum in the flow direction of molecules. TMAC has been experimentally measured

*hiroki@nagoya-u.jp

by several approaches using the velocity slip phenomenon, typically, the mass flow rate measurement in the slip flow regime and the measurement using the spinning rotor gauge [8–10]. By comparing the theoretical and measured values, TMAC is deduced from the viscous slip coefficient.

From the measurements of the accommodation coefficients, it appeared that EAC and TMAC showed different characteristics on the molecular mass of the gas species: By increasing the molecular mass, EAC drastically increases [2,3,6,7], whereas there were contrary results on TMAC: it slightly decreases [11,12] or slightly increases [13]. Even though the same gas species-surface material pair was employed, there remains a considerable variation in the measured values of EAC and TMAC [3,8,9]. If we focus only on the qualitative characteristics of the accommodation coefficients, there is the opposite tendency for EAC and TMAC, where the reason is not clear. Adding to that, there is an argument about the contrary results of the TMAC measurements. It is, however, not easy to reveal the characteristics of the accommodation coefficients by measurements, and there are several numerical studies employing the molecular dynamics method to investigate the gas-surface interaction [14–20]. It is important to note that it is difficult to simulate quantitatively an experimental result by the molecular dynamics simulations, because surface conditions for the whole surface area at the measured condition, like a roughness and adsorbed molecules, are not enough clear. Surface conditions are not easy to measure *in situ*, and it is also difficult to employ a defined clean bare surface in the atomic level in measurements. Therefore, the qualitative characteristics of the accommodation coefficients have been studied numerically. The effect of gas-surface interaction potential on TMAC was parametrically studied in Ref. [14], but it employed a surface with an rigid lattice corresponding to $T_s = 0$ and it is impossible in principle to study EAC by their framework. The dependence of TMAC on the molecular mass was studied in Ref. [20]. However, unfortunately TMAC in that study was based on individual molecules rather than bulk flow, which is different from the measurement because TMAC was measured by using the bulk flow as explained above; it is not adequate to discuss the experimental results by TMAC based on individual molecules. Moreover, there is another question of whether it is possible to employ EAC or TMAC for a thermo-fluid dynamics field where both heat transfer and flow exist.

In this study, the characteristics of EAC and TMAC based on the same definition with the measurements are investigated by the molecular dynamics method. In a numerical simulation, the natures of gas species, namely the molecular mass and the parameters of the gas-surface interaction potential, are parametrically studied to reveal the reason for the characteristics on the accommodation coefficients, which is one of the advantages of the numerical approach compared to the experimental measurements. Although it is well known that reproducing a real engineering surface on an atomic scale within a framework of the molecular dynamics study is not easy, due to a roughness, adsorbed molecules, and so on, it is possible to obtain a qualitative characteristics on the gas-surface interaction. The characteristics of the accommodation coefficients are qualitatively discussed from the results of the parametric study. To understand the physical mechanism of the characteristics easily, a simple potential model is employed. EAC and TMAC of a thermo-fluid dynamics field is studied and compared with EAC obtained from a static fluid and TMAC obtained from a thermal equilibrium flow.

II. NUMERICAL SIMULATION

There have been several molecular dynamics studies on the accommodation coefficients. Nanochannels were often employed to investigate gas-surface interaction [15,17–19]. Sometimes the direct simulation Monte Carlo (DSMC) method [21] was employed to simulate the bulk flow inside the channel [16]. It is, however, not clear that the conditions of incoming molecules to a surface are in equilibrium as in the experimental measurements due to a narrow nanochannel, compared with the conditions in experiments. Adding to that, it is questionable whether it is appropriate to obtain EAC from a thermally equilibrium flow and TMAC from a heat transfer through a static fluid, where EAC and TMAC were typically measured from a heat transfer and a mass flow rate, respectively. This is because it is clearly inadequate to consider EAC in a thermal equilibrium system or TMAC in a static fluid from the definitions, Eqs. (2) and (3); temperatures of gas and surface are the same, $\overline{E_i} = \overline{E_s}$, for the former case, and there is no specific direction for incident molecules in average, $\overline{p_{t,i}} = 0$, for the latter. It is noteworthy that the overline is an average over all molecules in the scattering process, and the above conditions are inevitably satisfied if the number of molecular samples is enough large. Thus, it is inadequate to use the velocities of scattering gas molecules without averaging [19]. It could be also different from experimental results that use an accommodation coefficient based on an individual molecule [20].

Based on these points, we employed a different approach to obtain the accommodation coefficients by the molecular dynamics simulation in this study: An individual process of a gas molecule coming to, colliding with, and scattering from a surface was simulated [14,20] based on the molecular dynamics code employed in Refs. [22–24]. In other words, gas molecules were simulated just from the last collision to another gas molecule before colliding with a surface until the next collision after the scattering. This approach was similar to the previous studies using nanochannels in the sampling process to calculate accommodation coefficients, since properties of gas molecules before and after collisions to calculate the accommodation coefficients were usually sampled at the distance determined by the mean free path from a surface. It is therefore important to note that the scattering process of each molecule can be separately analyzed because of the independent processes, resulting in adaptability to the parallel computation and the reduction of the computational cost. This allows us the advantage of simulating a large number of trajectories to calculate the accommodation coefficients statistically.

The incident conditions were determined by the equilibrium theoretical velocity distribution to represent the conditions of a bulk fluid [14]. In the measurements, although EAC was often measured in the free-molecular flow regime, the conditions of incoming molecules were well determined to be a thermal equilibrium condition. TMAC was often measured in the slip

flow regime, where gas molecules experience many collisions with other gas molecules. Therefore, it is reasonable to assume the equilibrium condition to represent the measurements. This approach enables us to evaluate EAC and TMAC within the same framework; to calculate EAC from a heat transfer through a static fluid and TMAC from a thermally equilibrium flow, just the velocity distributions, which determine the incident conditions, were changed. Gas molecules impinging on a surface within an equilibrium bulk fluid follow the velocity distribution of the Maxwell distribution for a static gas and the shifted Maxwell distribution for a gas with a macroscopic bulk flow velocity of u. The distributions are expressed as

$$f = \frac{m}{2\pi k T_g} \exp\left\{-\frac{m}{2kT_g}\left[(c_x - u)^2 + c_y^2\right]\right\} \cdot \frac{m}{kT_g} c_z \exp\left[-\frac{m}{2kT_g} c_z^2\right], \quad (4)$$

where c_i are molecular velocity of each component, m is the molecular mass, and T_g is the temperature of gas. The x axis was the direction of the bulk flow, which was parallel to a surface, and the z axis was normal to the surface. The distribution with $u = 0$ is called the Maxwell and $u \neq 0$ the shifted Maxwell distributions. Therefore, the incident velocities were stochastically sampled from this velocity distribution function, Eq. (4); $u = 0$ for EAC and $u \neq 0$ for TMAC.

A monatomic Lennard-Jones molecule was employed as the gas species. The characteristics of the accommodation coefficients were studied by changing the molecular parameters of the mass of a gas molecule m_g and the parameters of the Lennard-Jones (12-6) gas-surface interaction potential, ϵ_{gs} and σ_{gs}, one by one. The trajectories of a gas molecule and surface atoms were calculated solving the Newton's equations of motions by the velocity Verlet algorithm, where the time step was 1.85 fs. The surface was modeled by a slab with the Miller index of (111) of three layers of 392 atoms in each layer, whose size was 3.33 × 3.36 nm. The interaction between surface atoms were also represented by the Lennard-Jones (12-6) potentials with the parameters of $\epsilon_s = 3772$ K and $\sigma = 0.247$ nm, i.e., Pt atoms [18]. The slab in a thermal equilibrium at the surface temperature $T_s = 300$ K was prepared beforehand after simulating 0.2 ns with temperature control and 0.8 ns without temperature control. The periodic boundary conditions were applied to the x-y plane. This prepared slab was loaded as the initial condition of surface atoms at every scattering process simulation. However, to avoid the same surface condition for different incident gas molecules, the slab was randomly rotated and every gas molecule was initially placed at a randomly selected position in the xy plane at the height of $z_i = 6\sigma_{gs}$ from a surface, which was equal to the cutoff distance of the potential. The initial velocities of gas molecules were stochastically sampled from the Maxwell or the shifted Maxwell distribution using the method often employed in the DSMC [21]. To evaluate EAC, the Maxwell distribution, Eq. (4) with $u = 0$, with the temperature of gas $T_g = 250$ K, where the temperature difference between gas and surface was $\Delta T = 50$ K, was employed. To evaluate TMAC, the shifted Maxwell distribution, Eq. (4) with $u = 0.1C_{mp}$,

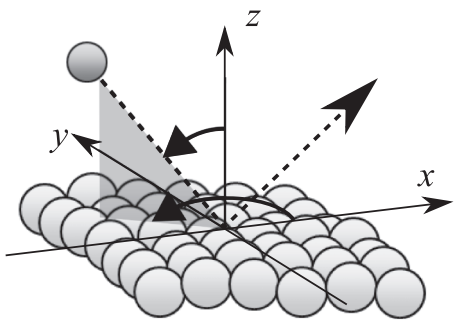

FIG. 1. A numerical coordinate system.

where $C_{mp} = \sqrt{\frac{2kT}{m}}$, with the temperature of gas $T = 300$ K, was employed. The initial incident velocity vectors, namely the position of a gas molecule in Fig. 1, are plotted in Fig. 2. From the figures, the incident velocity vectors were widely scattered, and those for TMAC were slightly biased toward $x < 0$ region because of $u > 0$. A gas molecule impinged on the surface one at a time in every simulation, and the simulation was continued until the gas molecule escaped in the height more than z_i away from the surface. If the total energy of a gas molecule was lower than $2kT_s$ or the simulation reached 66 666 steps (123 ps), the gas molecule was determined to be trapped. These trapped molecules were estimated to have properties fully accommodated to the surface condition after the collision. For each incidence condition, 10 000 trajectories were simulated.

III. RESULTS AND DISCUSSION

A. Accommodation coefficients

First, the energy accommodation coefficient (EAC), Eq. (2), and the tangential momentum accommodation coefficient (TMAC), Eq. (3), were calculated from the simulated trajectories for noble gases: He, Ne, Ar, and Kr. The interaction potential parameters (σ_{gs}, ϵ_{gs}) were determined based on the value of Pt-Ar [17,18] and relatively evaluated by the Lorentz-Berthelot rules using the parameters of gas molecules in Refs. [25,26] as (2.38 Å, 23.093 K) for He, (2.60 Å, 49.572 K) for Ne, (2.94 Å, 79.144 K) for Ar, and (3.15 Å, 92.600 K) for

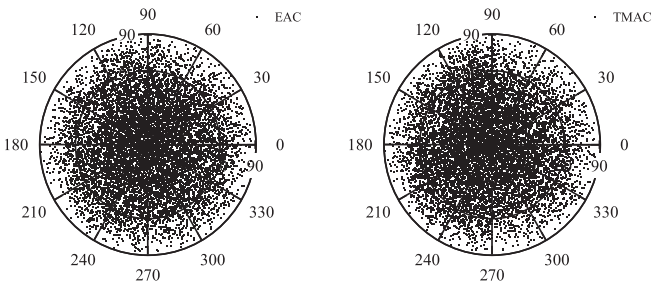

(a) EAC (b) TMAC

FIG. 2. The initial incident velocity vectors towards colliding points for gas molecules are plotted. They are sampled from the Maxwell distribution for EAC and the shifted Maxwell distribution in the x direction for TMAC.

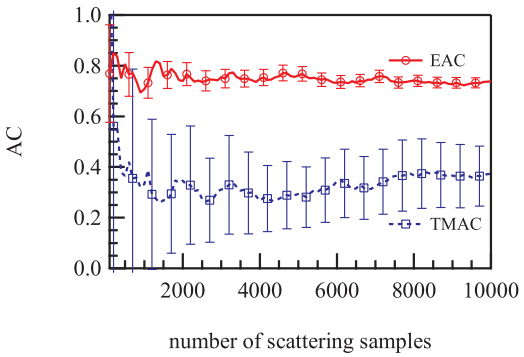

FIG. 3. Typical convergences of EAC and TMAC against the number of scattering samples.

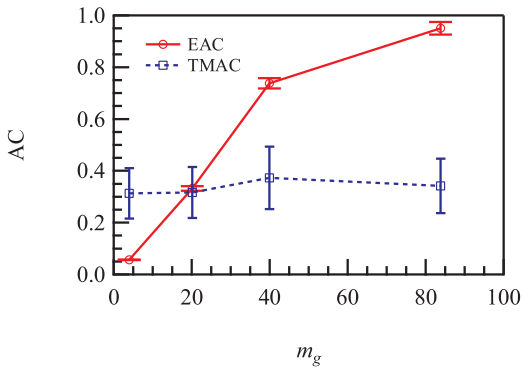

FIG. 4. The calculated EAC and TMAC for He, Ne, Ar, and Kr are plotted against the molecular weight.

Kr, respectively, where the parameter for Xe is not listed. Thus, the parameters for Pt-Ar were the same with Refs. [17,18].

The convergences of EAC and TMAC are plotted for Ar as a function of the number of the scattering samples n in Fig. 3. The 95% confidence interval for TMAC is still large even with the number of sample $n = 10\,000$ compared with EAC. It is understandable since the size of the velocity, i.e., speed, is involved in EAC, whereas TMAC focuses on the x component of the velocity and needs a large number of samples to have the same confidence interval. It could be enough, however, to check the qualitative tendency of the characteristics even for TMAC.

Before analyzing the accommodation coefficients, the simulation was validated by comparing the obtained values with those in the literature, since there is a discrepancy between the values by the molecular dynamics studies and the experiments. For the validation, EAC by Ref. [17] and TMAC by Ref. [18] for Pt-Ar obtained by using nanochannels were employed; the simulated systems were different from our simulation, though the same potentials were used. It is important to note that the molecules determined as trapped in our study are evaluated as fully accommodated to the surface to reduce the computational cost. Therefore, we omit the trapped molecules from the calculation of the accommodation coefficients here. EACs obtained by the two parallel plates with the temperatures at 150 K and 300 K were 0.43 and 0.37, respectively [17], while we obtained EAC at $T_g = 200$ K as 0.46. For TMAC, our simulation is only limited to the colliding process, which would correspond to the large Knudsen number. TMAC obtained by the acceleration-field-driven Poiseuille flow were 0.313–0.247 for $Kn = 0.72$ depending on the magnitude of the acceleration [18], whereas TMAC was calculated as 0.34 in our simulation. Since the simulated conditions were not exactly the same, they showed quite good agreement.

The obtained accommodation coefficients for noble gases are plotted in Fig. 4 with confidence intervals. From Fig. 4, EAC is strongly dependent on the molecular mass and increases with increasing the molecular mass, whereas TMAC is almost constant. Comparing the result with the experimental values, there is a quantitative discrepancy both for EAC and TMAC, as mentioned in the introduction. However, the tendency of EAC is the same as that in the measurements [6,7], where EAC drastically increases from He to Xe. For TMAC, the variation of the values among noble gases is much smaller compared with EAC. Comparing with the results in the literature, TMAC shows the trend in between the slightly increasing result [13] and the slightly decreasing results [11,12], which is reasonable considering the large confidence intervals. Compared with the previous molecular dynamics study [20], the increase from He to Ne is not observed in Fig. 4. This could be because the shifted Maxwell distribution and TMAC of the bulk flow are employed and the surface material is Pt in this study rather than Si as in the literature.

B. Parametric study

1. Parameters

In the previous section, we evaluated the accommodation coefficients between several noble gas species. However, the reason for the tendency of the accommodation coefficients is still not clear. It is often the case to use the molecular mass to order the gas species, but we can obtain a similar trend by plotting against another parameter, like the viscosity and the thermal conductivity, since they are strongly correlated for the noble gas species. Thus, a parametric study is used to understand the effect of the parameters on the accommodation coefficients [14], which was only possible in the numerical study.

The parameters for the scattering process of a gas molecule from a surface are the ratio of molecular mass between gas and surface m_g/m_s and the parameters of the gas-surface interaction potential ϵ_{gs} and σ_{gs}. These parameters depend on both a gas molecule and surface atoms. In this study, the parameters of surface atoms were fixed to the values corresponding to Pt, while those of a gas molecule were varied; three parameters of the molecular mass of gas m_g and the interaction potential parameters ϵ_{gs} and σ_{gs} were changed one by one. The interaction parameters between surface atoms ϵ_s and σ_s were not considered as parameters. If ϵ_s is varied, the strength of surface atoms' network is varied, and the number of atoms to be affected by an incident gas molecule is varied. If surface atoms within a large area are affected, it could be similar to the scattering process with heavy surface atoms, and vice versa; i.e., the effect from ϵ_s is similar to that from the mass of surface atoms m_s. σ_s corresponds to the size of surface atoms and the only important value is the ratio of σ_s to σ_g. Therefore, the effect of σ_s is the same with that of σ_{gs}. The parameters of the base condition were selected as those for

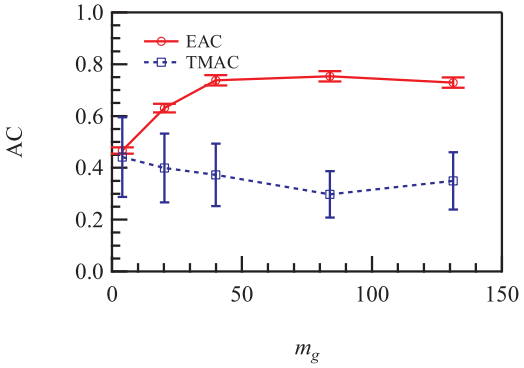

FIG. 5. The calculated EAC and TMAC, changing only the molecular mass m_g artificially.

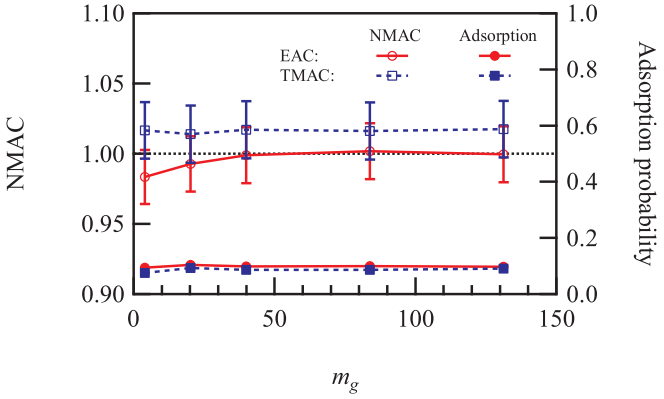

FIG. 6. The calculated NMAC (left axis) and adsorption probability (right axis), changing only the molecular mass m_g artificially.

Ar: $m_g = 39.95$ amu, $\epsilon_{gs} = 79.144$ K, and $\sigma_{gs} = 0.294$ nm. The parameters were varied among the values of noble gases separately. The molecular mass m_g was chosen among He (4.003), Ne (20.18), Ar (39.95), Kr (83.80), and Xe (131.3). To compensate for the lack of data for Xe and to clarify tendencies by increasing the range of parameters, the pair of the potential parameters were chosen from a little extended range based on the values for these noble gases; ϵ_{gs}[K] was chosen among 10.000, 23.093 (He), 49.572 (Ne), 79.144 (Ar), 92.600 (Kr), and 120.00, and σ_{gs}[Å] was chosen among 2.00, 2.38 (He), 2.60 (Ne), 2.94 (Ar), 3.15 (Kr), and 3.50. When one parameter was changed, the other parameters were fixed to the base condition of Ar.

2. *Molecular mass m_g*

The obtained results for varying the molecular mass of gas are plotted in Fig. 5. As seen from Fig. 5, EAC increases with increasing the molecular mass where $m_g < 40$, while it is nearly constant for heavier gases. TMAC slightly decreases with increasing the molecular mass.

To investigate this in detail, the interaction in the normal direction was analyzed by employing the normal momentum accommodation coefficient (NMAC). There are several definitions for NMAC [9]; in this study, we employed the definition [27] as

$$\alpha_n = \frac{\overline{p_{n,i}} - \overline{p_{n,r}}}{\overline{p_{n,i}} - \overline{p_{n,s}}} = \frac{|\overline{p_{n,i}}| + |\overline{p_{n,r}}|}{|\overline{p_{n,i}}| + |\overline{p_{n,s}}|}, \tag{5}$$

where p_n denotes the normal momentum of gas molecules, and $\overline{p_{n,s}} = m_g\sqrt{\frac{\pi}{2}\frac{kT}{m_g}}$. Note that incoming $p_{n,i}$ and scattering $p_{n,r}$, $p_{n,s}$ are in opposite directions. NMAC and the adsorption probability are plotted in Fig. 6. From the figure, NMAC has nearly the same trend as the accommodation coefficients in Fig. 5. A heavier gas molecule is easier to accommodate to the surface, since the mean velocity of heavier gas molecules is smaller at the same temperature and the duration to be influenced by the gas-surface interaction is longer. By increasing the molecular mass, the EAC increases. For the EAC condition, NMAC reaches unity at $m_g \geqslant 40$; gas molecules are fully accommodated in the normal direction. This could be the reason it is constant at $m_g > 40$. Even though gas molecules completely accommodate in the normal direction, they do not accommodate in the tangential direction estimated from TMAC in Fig. 5, resulting in EAC $\alpha_E < 1$. This threshold could be determined by the balance between the molecular mass and the interaction strength to accommodate to the surface, which corresponds to the condition of Ar in this study. For TMAC, a heavier gas molecule tends to keep the tangential momentum by their inertia, while the accommodation process changes the normal component of the velocity. Therefore, the scattering angle distribution resulting from their balance could slightly affect the value of TMAC.

3. *Interaction strength ϵ_{gs}*

The interaction strength of the Lennard-Jones potential between gas and surface ϵ_{gs} was varied and the results are plotted in Fig. 7. The tendency of TMAC is similar to that in Ref. [14]. For ϵ_{gs}, EAC and TMAC show the same tendency. NMAC and the adsorption probability in Fig. 8 also increase. This is reasonable because molecules accommodate to the surface by increasing the interaction strength. For the condition of $\epsilon_{gs} = 120$ K, the interaction strength could be too strong compared to the mass ratio of a gas molecule to a surface atom to show EAC more than unity, because of the artificial parameter setting.

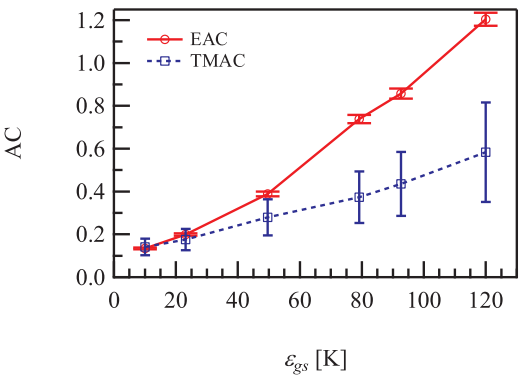

FIG. 7. The calculated EAC and TMAC by changing only the interaction strength between gas and surface ϵ_{gs} artificially.

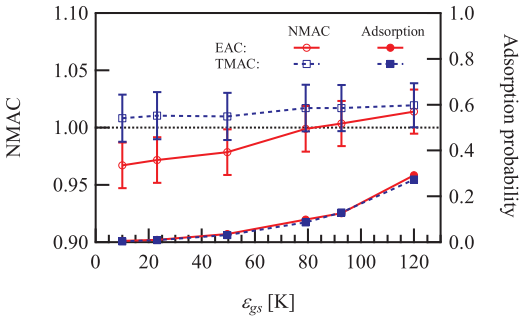

FIG. 8. The calculated NMAC (left axis) and adsorption probability (right axis) by changing only the interaction strength between gas and surface ϵ_{gs} artificially.

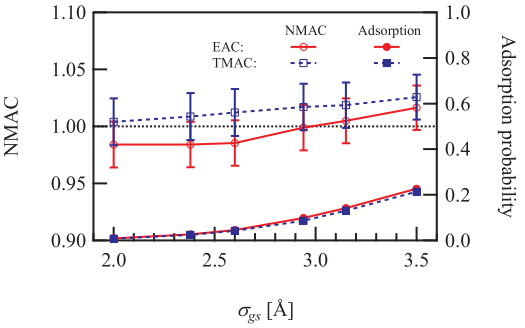

FIG. 10. The calculated NMAC (left axis) and adsorption probability (right axis), changing only the size of a gas molecule σ_{gs} artificially.

4. *Molecular size σ_{gs}*

σ_{gs} represents the relative size of a gas molecule to surface atoms. By decreasing σ_{gs}, a gas molecule becomes relatively smaller; thus, the surface becomes corrugated from the viewpoint of a gas molecule. The surface is relatively flat by increasing σ_{gs}. Therefore, this parameter represents the effect from surface roughness in the scattering process.

From Fig. 9, the trends of EAC and TMAC are opposite. The tendency of TMAC is similar to that in Ref. [14]. By checking NMAC and the adsorption probability in Fig. 10, it is interestingly nearly the same result with the interaction strength ϵ_{gs} in Fig. 8. Thus, energy is more transferred between gas and surface by increasing σ_{gs} due to the increase in the normal momentum transfer. This could be because the number of surface atoms involved in the scattering process, namely in the distance of several σ_{gs} from a gas molecule where the attraction force exists, is larger for a flat surface than for a corrugated surface. TMAC decreases with increase in σ_{gs}, which is contradictory to the result for ϵ_{gs} in Fig. 7, even though NMAC and the adsorption probability have trends similar to Fig. 8. This behavior could be coming from the scattering distribution of gas molecules, and the scattered angle distribution was investigated. The intensity distributions of TMAC against the scattering angle for the polar angle from x axis, which is coincident with the bulk flow direction $\vec{u}$, are plotted for the smallest $\sigma_{gs} = 2.0$ Å and for the largest $\sigma_{gs} = 3.5$ Å conditions in Fig. 11. It is shown that the scattering intensity in the positive x direction, i.e., the flow direction, increases with increasing σ_{gs}; the component similar to the mirror scattering increases with the surface flatness. In other words, the corrugation increases the probability of the back-scattering process, and TMAC increases with decreasing the flatness of the surface.

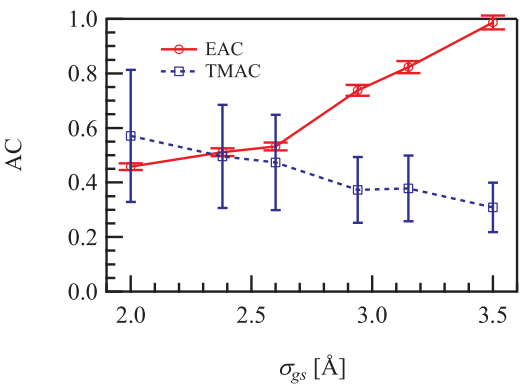

FIG. 9. The calculated EAC and TMAC, changing only the size of a gas molecule σ_{gs} artificially.

5. *EAC and TMAC*

The characteristics of EAC and TMAC appear to be different based on the influence of the parameters. EAC increases by increasing every parameter, because of the transfer in the normal direction. TMAC decreases with increasing m_g and σ_{gs}, but it increases with increasing ϵ_{gs}. This is because TMAC is strongly influenced by the scattering angle distribution. Therefore, considering that all the parameters increase by changing the gas species from He to Kr, it is reasonable that EAC increases drastically by the superposition of the effects from all parameters, while TMAC remains nearly constant because of the compensation of the effects.

In the experimental results, almost all the results of EAC show the same tendency for the gas species, while there were several contradictory results for TMAC. This could be because the dependencies on m_g, σ_{gs}, and ϵ_{gs} are opposite

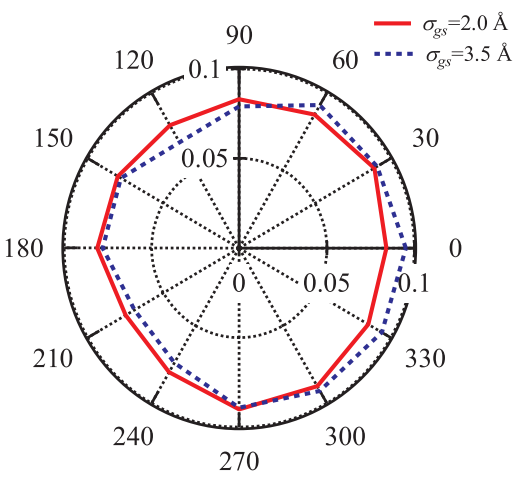

FIG. 11. The scattering polar angle distributions of TMAC for the smallest $\sigma_{gs} = 2.0$ Å and for the largest $\sigma_{gs} = 3.5$ Å conditions.

only in TMAC. In the measurements, the surface conditions were totally different from the defined clean bare surface in the atomic level used in this study. There could be surface roughness and/or adsorbed molecules for the surfaces employed in the experiments. If we consider effective values of the potential parameters for such real surfaces employed, the parameters could be different from one surface to another. TMAC could be slightly increased by the effect of effective ϵ_{gs} component, while slightly decreased by the effects of effective m_g and σ_{gs} components. Therefore, we can conclude that the difference in the surface condition led to the controversial results in the experiments.

C. Bulk flow and heat transfer

In high Knudsen number flows, the thermal creep (thermal transpiration) flow [28–31] is induced by the temperature gradient on a surface. In such a case, macroscopic bulk flow and heat transfers to/from a surface coexist, and it is different from the condition for obtaining either EAC or TMAC in this study, since $u \neq 0$ at the same time as $T_g \neq T_s$. Therefore, there remains a question as to whether EAC or TMAC could be employed to simulate such a flow.

To check EAC and TMAC for the condition of a thermo-fluid dynamics field and investigate the difference from EAC for a static fluid or TMAC for a thermal equilibrium flow obtained in the previous section, EAC and TMAC for He, Ne, Ar, and Kr were obtained by using the shifted Maxwell distribution with both the bulk flow $u \neq 0$ and the temperature difference between gas and surface $\Delta T \neq 0$. They are plotted against the molecular weight in Fig. 12 by the legend "with ΔT & u", compared with original EAC and TMAC. From the figure, it can be seen that EAC is nearly the same as the original case of a static fluid while TMAC is slightly larger than the original case of a thermal equilibrium flow. NMAC in Fig. 13 shows that the momentum transfer in the normal direction is almost the same with the condition of the original EAC condition, where the condition for the original EAC simulation and the original TMAC simulation is shown by the legends "with ΔT" and "with u", respectively. The transfer between gas and surface in the normal direction can be estimated to be mainly concerned with the heat transfer as

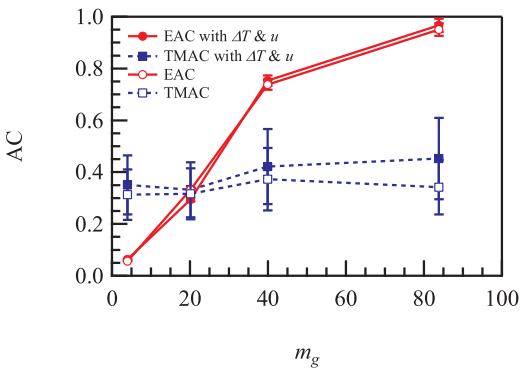

FIG. 12. The EAC and TMAC for He, Ne, Ar, and Kr are obtained by using the shifted Maxwell distribution with the bulk flow $u \neq 0$ and the temperature difference between gas and surface $T_g \neq T_s$, and they are plotted against the molecular weight.

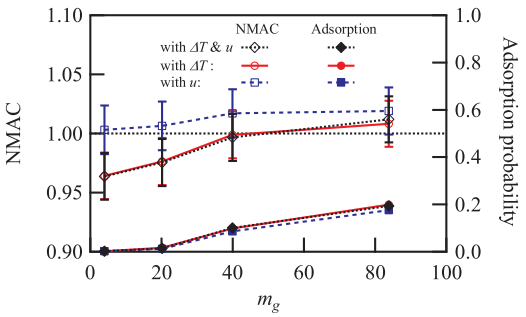

FIG. 13. The calculated NMAC (left axis) and adsorption probability (right axis) by using the shifted Maxwell distribution with the bulk flow $u \neq 0$ and the temperature difference between gas and surface $T_g \neq T_s$.

in Sec. III B. The effect from the heat transfer coming from the temperature difference between gas and surface $\Delta T = 50\,\mathrm{K}$ is much larger than that from the bulk flow $u = 0.1C_{mp}$. Their balance could be different depending on the size of ΔT and u; however, the effect of the temperature difference ΔT could be dominant. Because of the momentum transfer in the normal direction, the degree of accommodation could increase and TMAC could also increase compared to the original thermal equilibrium flow condition. From these results, in our simulated conditions, the bulk flow seems to be affected by the temperature difference between gas and surface, whereas the heat transfer problem seems to hardly be affected by the bulk flow. Therefore, the use of TMAC in flow analysis of the thermo-fluid dynamic fields would requires considerable attention.

IV. CONCLUSION

The molecular dynamics study was employed to investigate the characteristics of the accommodation coefficient. The energy accommodation coefficient (EAC) and the tangential momentum accommodation coefficient (TMAC) were calculated from a large number of trajectories of gas molecules colliding to and scattering from a surface, using the simple definition. To replicate the experimental measurements on a larger scale compared to the size of the molecular dynamics study, the incident velocities were stochastically sampled from the equilibrium velocity distributions; the Maxwell distribution with a different temperature from the surface was employed for EAC and the shifted Maxwell distribution was used for TMAC. The obtained tendency of EAC and TMAC for noble gases were qualitatively coincident with the experimental results. To understand the characteristics in detail, EAC and TMAC were parametrically studied by changing the molecular mass of gas, the interaction strength between gas and surface and the molecular size of gas one by one artificially. From the parametric study, EAC increased with increasing every parameter, while TMAC increased with increasing interaction strength, but TMAC decreased with increasing molecular mass and molecular size of gas. It is not so surprising that TMAC for noble gases showed the opposite tendency in the experimental measurement from these characteristics. Even though the surface materials were

the same, the surface conditions were not always the same. The difference between the surface conditions in the balance among the effective molecular mass, interaction strength, and molecular size, which were determined by considering the effects from surface roughness and/or adsorbed molecules, could result in the contrary results. EAC and TMAC for thermo-fluid dynamics field under the condition with the temperature difference between gas and surface and the bulk flow at the same time were also investigated. In the simulated conditions, EAC was nearly the same as the static fluid case, whereas TMAC seemed to increase slightly compared with the thermal equilibrium case.

[1] F. Sharipov, J. Phys. Chem. Ref. Data **40**, 023101 (2011).

[2] F. O. Goodman and H. Y. Wachman, *Dynamics of Gas-Surface Scattering* (Academic Press, New York, 1976).

[3] S. C. Saxena and R. K. Joshi, *Thermal Accommodation and Adsorbtion Coefficients of Gases* (Hemisphere Publishing, New York, 1989).

[4] W. M. Trott, J. N. Castañeda, J. R. Torczynski, M. A. Gallis, and D. J. Rader, Rev. Sci. Instrum. **82**, 035120 (2011).

[5] H. Yamaguchi, K. Kanazawa, Y. Matsuda, T. Niimi, A. Polikarpov, and I. Graur, Phys. Fluids **24**, 062002 (2012).

[6] H. Yamaguchi, T. Imai, T. Iwai, A. Kondo, Y. Matsuda, and T. Niimi, J. Vac. Sci. Technol. A **32**, 061602 (2014).

[7] H. Yamaguchi, M. T. Ho, Y. Matsuda, T. Niimi, and I. Graur, Inter. J. Heat Mass Transf. **108**, 1527 (2017).

[8] A. Agrawal and S. V. Prabhu, J. Vac. Sci. Technol. A **26**, 634 (2008).

[9] B.-Y. Cao, J. Sun, M. Chen, and Z.-Y. Guo, Int. J. Mol. Sci. **10**, 4638 (2009).

[10] H. Yamaguchi, T. Hanawa, O. Yamamoto, Y. Matsuda, Y. Egami, and T. Niimi, Microfluidic. Nanofluidic. **11**, 57 (2011).

[11] P. Perrier, I. A. Graur, T. Ewart, and J. G. Méolans, Phys. Fluids **23**, 042004 (2011).

[12] H. Yamaguchi, K. Takamori, P. Perrier, I. Graur, Y. Matsuda, and T. Niimi, Phys. Fluids **28**, 092001 (2016).

[13] B. T. Porodnov, P. E. Suetin, S. F. Borisov, and V. D. Akinshin, J. Fluid Mech. **64**, 417 (1974).

[14] G. Arya, H.-C. Chang, and E. J. Maginn, Mol. Simul. **29**, 697 (2003).

[15] B. Y. Cao, M. Chen, and Z. Y. Guo, Appl. Phys. Lett. **86**, 091905 (2005).

[16] K. Yamamoto, H. Takeuchi, and T. Hyakutake, Phys. Fluids **18**, 046103 (2006).

[17] P. Spijker, A. J. Markvoort, S. V. Nedea, and P. A. J. Hilbers, Phys. Rev. E **81**, 011203 (2010).

[18] S. K. Prabha and S. P. Sathian, Phys. Rev. E **85**, 041201 (2012).

[19] Z. Liang and P. Keblinski, Inter. J. Heat Mass Transf. **78**, 161 (2014).

[20] W. W. Lim, G. J. Suaning, and D. R. McKenzie, Phys. Fluids **28**, 097101 (2016).

[21] G. A. Bird, *Molecular Gas Dynamics and the Direct Simulation of Gas Flows* (Oxford University Press, New York, 1994).

[22] Y. Watanabe, H. Yamaguchi, M. Hashinokuchi, K. Sawabe, S. Maruyama, Y. Matsumoto, and K. Shobatake, Chem. Phys. Lett. **413**, 331 (2005).

[23] Y. Watanabe, H. Yamaguchi, M. Hashinokuchi, K. Sawabe, S. Maruyama, Y. Matsumoto, and K. Shobatake, Euro. Phys. J. D **38**, 103 (2006).

[24] H. Yamaguchi, K. Shobatake, and T. Niimi, in *Rarefied Gas Dynamics: Proceedings of the 26th International Symposium on Rarefied Gas Dynamics*, AIP Conf. Proceed. No. 1084 (AIP, New York, 2008), p. 647.

[25] M. P. Allen and D. J. Tildesley, *Computer Simulation of Liquids* (Clarendon, Oxford, UK, 1987).

[26] G. C. Maitland, M. Rigby, E. B. Smith, and W. A. Wakeham, *Intermolecular Forces: Their Origin and Determination* (Clarendon, Oxford, UK, 1981).

[27] S.-M. Liu, P. K. Sharma, and E. L. Knuth, AIAA J. **17**, 1314 (1979).

[28] B. T. Porodnov, A. N. Kulev, and F. T. Tuchevetov, J. Fluid Mech. **88**, 609 (1978).

[29] M. Rojas-Cárdenas, I. Graur, P. Perrier, and J. G. Méolans, Phys. Fluids **23**, 031702 (2011).

[30] H. Yamaguchi, M. Rojas-Cárdenas, P. Perrier, I. Graur, and T. Niimi, J. Fluid Mech. **744**, 169 (2014).

[31] H. Yamaguchi, P. Perrier, M. Ho, J. Méolans, T. Niimi, and I. Graur, J. Fluid Mech. **795**, 690 (2016).